THE JOURNAL OF PHYSICAL CHEMISTRY B

Article

pubs.acs.org/JPCB

Diffusion-Enhanced Förster Resonance Energy Transfer and the Effects of External Quenchers and the Donor Quantum Yield

Maik H. Jacob,* Roy N. Dsouza,† Indrajit Ghosh,† Amir Norouzy, Thomas Schwarzlose, and Werner M. Nau*

School of Engineering and Science, Jacobs University Bremen, Campus Ring 1, D-28759, Bremen, Germany

Supporting Information

ABSTRACT: The structural and dynamic properties of a flexible peptidic chain codetermine its biological activity. These properties are imprinted in intrachain site-to-site distances as well as in diffusion coefficients of mutual site-to-site motion. Both distance distribution and diffusion determine the extent of Förster resonance energy transfer (FRET) between two chain sites labeled with a FRET donor and acceptor. Both could be obtained from time-resolved FRET measurements if their individual contributions to the FRET efficiency could be systematically varied. Because the FRET diffusion enhancement (FDE) depends on the donor-fluorescence lifetime, it has been proposed that the FDE can be reduced by shortening the donor lifetime through an external quencher. Benefiting from the high diffusion sensitivity of short-distance FRET, we tested this concept experimentally on a $(Gly–Ser)_6$ segment labeled with the donor/acceptor pair naphthylalanine/2,3-diazabicyclo[2.2.2]-oct-2-ene (NAla/Dbo). Surprisingly, the very effective quencher potassium iodide (KI) had no effect at all on the average donor–acceptor distance, although the donor lifetime was shortened from ca. 36 ns in the absence of KI to ca. 3 ns in the presence of 30 mM KI. We show that the proposed approach had to fail because it is not the experimentally observed but the radiative donor lifetime that controls the FDE. Because of that, any FRET ensemble measurement can easily underestimate diffusion and might be misleading even if it employs the Haas–Steinberg diffusion equation (HSE). An extension of traditional FRET analysis allowed us to evaluate HSE simulations and to corroborate as well as generalize the experimental results. We demonstrate that diffusion-enhanced FRET depends on the radiative donor lifetime as it depends on the diffusion coefficient, a useful symmetry that can directly be applied to distinguish dynamic and structural effects of viscous cosolvents on the polymer chain. We demonstrate that the effective FRET rate and the recovered donor–acceptor distance depend on the quantum yield, most strongly in the absence of diffusion, which has to be accounted for in the interpretation of distance trends monitored by FRET.

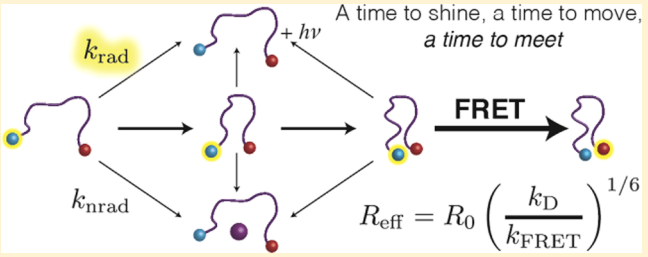

INTRODUCTION

Many bioactive peptides, proteins, and nucleic acids are too flexible to be fully accessible to traditional methods of structure elucidation. Examples are antimicrobial and cell-penetrating peptides, amyloidogenic peptides,[1,2] globular proteins in diverse stages of enzymatic catalysis as well as in diverse phases of refolding and unfolding and in the unfolded state,[3−10] and the large class of intrinsically disordered or natively unfolded proteins.[1,2,11] Nevertheless, every polypeptide chain shows distinct structural and dynamic patterns, which—if they were known—could assist in comprehending or even predicting biological activity.[12,13]

In this context, Förster resonance energy transfer (FRET) has increasingly come into focus. FRET from an energy donor dye to an acceptor dye, both conjugated to the chain at selected positions, is distance dependent and can thereby bring the sensitivity and speed of fluorescence spectroscopy to distance and structure determination of polypeptides (and nucleic acids).[3,4,14−24] Time-resolved FRET on the ensemble and also single-molecule FRET[25] offer the additional possibility to obtain information on the dynamic properties of the peptide chain, i.e., on intrachain diffusion; in general, this diffusion enhances FRET.[2,25] Unfortunately, although the analysis of time-resolved FRET data has been pioneered by Steinberg and Haas,[26−30] and expanded by Lakowicz and Kusba,[31−33] both experimental and computational challenges have arisen which have prevented it from becoming routine. The main roadblock is that the efficiency of FRET is determined by *both* chain structure and dynamics, that is, by the distance distribution of and by the mutual diffusion between two labeled chain positions. They can only be reliably delineated from time-resolved-fluorescence measurements if their relative contributions can be independently determined or, at least, systematically modified, in a series of experiments.[27]

Lakowicz and co-workers proposed an elegant idea to systematically reduce the FRET diffusion enhancement, the

Received: October 19, 2012
Revised: December 5, 2012
Published: December 6, 2012

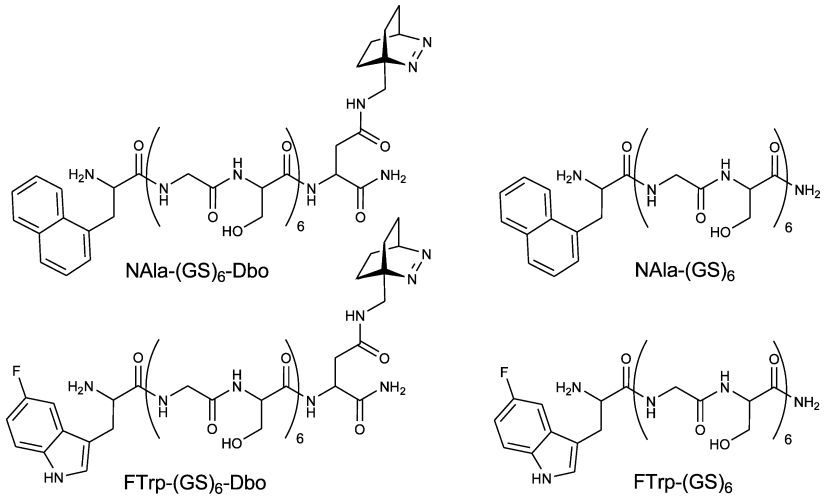

Figure 1. Selected donor–acceptor and donor-only labeled peptides composed of Gly–Ser units. Donors are naphthyl-1-L-alanine (NAla) and 5-fluoro-L-tryptophan (FTrp); the acceptor is Dbo, whose optically active group is the azo group of the bicyclic chromophore.

FDE, by addition of external quenchers.[34] Their idea was inspired by the random-walk perspective,[35] for which Lakowicz gave the following numerical example:[36] The possible root-mean-square (rms) donor–acceptor displacement, ΔR_{DA}, that can occur during the lifetime of the donor, τ_D, is obtained from $\Delta R_{DA} = (2D\tau_D)^{1/2}$.[36] ΔR_{DA} becomes 3.2 Å when the diffusion coefficient, D, is set to 1 Å^2/ns and the donor lifetime is set to 5 ns—a representative value for the experimental lifetimes of customary dyes. For a chain ensemble that displays an average distance of 20 Å, a displacement of 3.2 Å seems to be of limited significance. However, whenever a large displacement critically distorts the distance analysis, an external quencher can be added to the measurement solutions that, as proposed, reduces the donor lifetime and, by that, the displacement and the FDE.[34]

We will demonstrate that while the random-walk perspective grasps essential physical aspects of the FDE, it requires several modifications from the original idea. A minor correction, as already pointed out by others,[37] considers that mutual donor–acceptor diffusion takes place in three dimensions, leading to eq 1,[35] and results in an even larger rms displacement of 5.5 Å.

$$\Delta R_{rms} = (6D\tau_D)^{1/2} \quad (1)$$

More intriguingly, we will demonstrate that any donor lifetime reduction by a quencher cannot reduce the FDE. In fact, the donor lifetime to be inserted into eq 1 is the radiative and not the experimentally measured lifetime, which is often shorter by an order of magnitude. In the above example, the donor–acceptor displacement can then become as large as the average distance, exposing diffusion as an often dominant contributor to the FRET efficiency. As the impact of diffusion on FRET is much larger than has previously been assumed, other propositions of how to separately determine the distance distribution and the diffusion coefficient have to be revisited, too.[34,38]

To measure FDE experimentally, we will employ short-distance FRET,[39−43] i.e., FRET employing a donor–acceptor pair with a very short critical transfer distance of only 10 Å. This will allow us to follow the FDE with the highest resolution presently available.[40,42] On the theoretical level, we use known and introduce novel tools of elementary FRET analysis that will enable us to corroborate and generalize the experimental results by numerical simulations based on the Haas–Steinberg equation (HSE).[3,6,27,28,34,38] On our way, we have discovered critical aspects of FRET analysis that were never pointed out before.

MATERIALS AND METHODS

Donor-only and donor–acceptor labeled $(GS)_6$ peptides were obtained in higher than 95% purity from Biosyntan (Berlin). All peptides were amidated at the C terminus to exclude attractive interactions between the terminal positions. Fmoc-Dbo and 5-fluoro-L-tryptophan (FTrp) used in peptide synthesis were prepared according to literature methods.[44,45] Other chemicals were from Sigma-Aldrich. The ethylene glycol concentration was determined by refractive index measurement as previously described.[46,47] Absorption and fluorescence spectra were recorded on a Varian Cary 4000 UV–vis spectrometer and a Varian Cary Eclipse fluorometer. Time-resolved-fluorescence decays were followed by time-correlated single-photon counting with a FLS920 lifetime spectrometer (Edinburgh Instruments). A pulsed diode laser (Picoquant) was used for selective donor excitation at 280 nm. Peptide concentrations were determined by using extinction coefficients at 280 nm of 5.7×10^3 M^{-1} cm^{-1} (FTrp)[48] and 5.5×10^3 M^{-1} cm^{-1} (naphthylalanine, NAla)[49] and were adjusted to about 10 μM in aerated solutions at 25 °C and pH 5.0. The donor quantum yields were determined by comparison with *N*-acetyltryptophanamide (0.14, pH 7.0).[39,50,51] The Förster radii of NAla/Dbo and FTrp/Dbo were determined by using the absorption and emission spectra of the single-labeled peptides as previously described.[39,41] Fluorescence decays were analyzed by using the instrument software as described[39] and by using ProFit (Quantumsoft). The reproducibility of the reported fluorescence lifetimes for the monoexponential decays was ±3%. In the simulations, the HSE was solved numerically by using the finite element method implemented in the PDE toolbox of Matlab (MathWorks).

RESULTS

Short-Distance FRET Grants Maximal Diffusion Enhancement. Short-distance FRET employs donor–acceptor pairs with Förster radii of about 10 Å.[39−42,52] Thus, already a 1-Å diffusional displacement from a 10-Å donor–acceptor

dx.doi.org/10.1021/jp310381f | J. Phys. Chem. B 2013, 117, 185−198

distance increases the FRET efficiency and the donor decay rate to an extent that can be precisely determined.[40] Short-distance FRET is based on the acceptor Dbo, an asparagine residue conjugated to 2,3-diazabicyclo[2.2.2.]oct-2-ene (DBO). DBO's exceptionally small extinction coefficient causes a small spectral overlap of acceptor absorption and donor emission, which causes the observed short Förster radii.[39,42,52] The point–dipole approximation used in Förster's theory requires that the transition dipole vectors of donor and acceptor are much shorter than the distance between them.[53] The transition dipole of DBO is located on two atoms only, on the N=N group, which constitutes the azo chromophore. Quantum mechanical calculations on the Trp/DBO FRET pair yielded the conclusion that DBO as acceptor is a superior choice for short-distance detection.[52]

Previously, we have only used Trp as donor, but its intrinsic lifetime heterogeneity complicates data analysis.[39,54] In this work, we introduce two new FRET donors with mono-exponential fluorescence kinetics. The first, naphthyl-1-L-alanine (NAla), has an intrinsic lifetime of about 35 ns in aerated water and, thus, allows ample time for mutual donor–acceptor diffusion; the second, 5-fluoro-L-tryptophan (FTrp, Figure 1) has a lifetime of 2.0 ns, comparable to that of Trp with 1.4 ns.[55,56] Because all three donors, NAla, FTrp, and Trp, are virtually isosteric, the peptide chains (which differ only slightly in the donor structure) were expected to show identical structure and dynamics. Since Gly–Ser peptides have been shown to be highly flexible and have been investigated by a variety of methods, including FRET and collision-induced quenching,[38,39,44,57−61] we have selected a $(GS)_6$ sequence as the principal model, which afforded sizable FRET for all investigated peptides. For consistency, peptides of the sequence Donor-$(GS)_6$-Dbo were used (N-terminal donor and C-terminal acceptor) and the donor-only peptide, Donor-$(GS)_6$, was always included as a reference peptide for the donor decay in the absence of FRET (Figure 1).

Diffusion-Enhanced FRET Monitored through the Effective Donor–Acceptor Distance. Essential aspects of the impact of diffusion can already be accessed through a conventional FRET analysis. After optical excitation, the donor transfers its energy to the acceptor with a rate constant, k_T, which decreases with the sixth power of the donor–acceptor distance, R_{DA} (eq 2). Equation 2 is a central result of Förster theory and shows that the FRET rate depends also on the rate of donor deactivation, k_D, in the absence of the acceptor, that is, without competition by FRET. The Förster radius, R_0, is the donor–acceptor distance at which the FRET rate is as fast as deactivation by all non-FRET radiative and radiationless decay processes, including donor deactivation by an external quencher. The Förster radii were obtained from eq 3.[62] Here, the numerical constant $c = 9 \ln 10/(128\pi^5 N)$, with N being Avogadro's number.[63−65] The orientation factor, $\kappa^2 = 2/3$, assumes fast and random sampling of donor–acceptor orientations; this has been shown by molecular dynamics calculations to be a good approximation for the peptides under investigation.[39,41] The overlap integral, J, is determined by the extent by which the donor emission spectrum, normalized to an area of 1, i.e., $F_D(\lambda)$, overlaps with the spectrum, $\varepsilon(\lambda)$, of the acceptor absorption coefficient: $J = \int d\lambda F_D(\lambda)\ \varepsilon(\lambda)\ \lambda^4$. The Förster radius decreases with the refractive index, n, and increases with the donor quantum yield, Φ_D.

$$k_T = k_D(R_0/R_{DA})^6 \tag{2}$$

$$R_0^{\,6} = c\kappa^2 J \Phi_D / n^4 \tag{3}$$

The analysis is centered around the energy transfer efficiency (ETE), E, which is simply the fraction of donor-deactivation events, ΔN^*, caused by FRET; $E = \Delta N^*_{FRET}/\Delta N^*$. Thus, it is also the ratio of the FRET rate over the sum of all rates of donor deactivation (eq 4). The ETE depends only on the Förster radius and the donor–acceptor distance (eq 5), which is seen when k_T in eq 4 is substituted by the FRET distance law (eq 2). Once the Förster radius has been determined, the measured ETE gives access to R_{DA}.

$$E = k_T/(k_T + k_D) \tag{4}$$

$$E = R_0^{\,6}/(R_0^{\,6} + R_{DA}^{\,6}) \tag{5}$$

The ETE itself is determined from time-resolved-fluorescence measurements by assuming that the observed rate of deactivation in the donor–acceptor peptide, k_{DA}, is composed of the FRET rate and that of donor deactivation in the donor-only peptide: $k_{DA} = k_T + k_D$. Rate and time constants such as the donor lifetime are reciprocally related ($k_D = \tau_D^{-1}$), and both quantities are henceforth used interchangeably, This leads to eq 6, which is directly applicable in the case of monoexponential kinetics. In the case of more complex kinetics, amplitude-weighted lifetimes are used or, most straightforwardly, the areas under the decay curves (eq 7) are used as direct measures of the total fluorescence emitted by the donor-only or the donor–acceptor peptide.[39,54] The ETE can also be accessed through steady-state measurements of the fluorescence intensities, I (eq 8), at equal concentrations of donor-only and donor–acceptor labeled peptides. Of course, in the limit of a perfect experiment with infinitely fast temporal resolution (where no fluorescence can escape by being conceived as static in nature), the relative steady-state-fluorescence intensities (eq 8) and relative areas under the time-resolved-fluorescence decay curves (eq 7) should be the same.

$$E_{tr} = (\tau_D - \tau_{DA})/\tau_D \tag{6}$$

$$E_{tr} = (A_D - A_{DA})/A_D \tag{7}$$

$$E_{ss} = (I_D - I_{DA})/I_D \tag{8}$$

The R_{DA} value determined from the ETE (eq 5) is a realistic physical distance only if the donor–acceptor separation does not vary among the molecules of the ensemble and when it does not vary with time. These conditions are approximately met in folded single-domain proteins,[37] in short polyproline chains of rigid helical PPII conformation,[38] or in the solid state.[41,42] However, when the same elementary procedure is used to determine the donor–acceptor distance for a chain ensemble characterized by a probability distribution of static distances, $p(r)$, the observed ETE includes FRET contributions from the entire range of distances and follows $E_{obs} = \int E(r)\ p(r)\ dr$. Because the efficiency at a specific distance, $E(r)$, is much larger at short distances than at long distances, the effective distance, R_{eff}, calculated from the observed ETE (cf. eq 5) will always be shorter than the average ensemble distance.[42]

A much larger apparent distance distortion is usually caused by chain mobility, that is, by mutual donor–acceptor motion. While the donor resides in its excited state, its distance to the acceptor is lengthened and shortened by mutual diffusion. The measured ETE and the effective FRET rate derived from it (cf. eq 4) is raised because any motion toward shorter distance

dx.doi.org/10.1021/jp310381f | J. Phys. Chem. B 2013, 117, 185−198

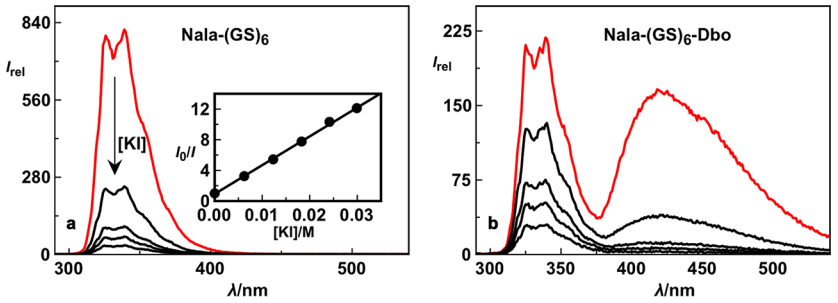

Figure 2. (a) Steady-state-fluorescence spectra of NAla-$(GS)_6$-NH_2 (λ_{exc} = 280 nm) in the absence (red trace) and presence (black traces) of increasing concentrations of potassium iodide (KI). Inset: The Stern–Volmer plot resulted in a quenching rate constant of $(10 \pm 1) \times 10^9$ M^{-1} s^{-1}. (b) Steady-state-fluorescence spectra of NAla-$(GS)_6$-Dbo in the absence (red trace) and presence (black trace) of KI. Note that the Dbo emission near 440 nm decreases even more rapidly with KI concentration than the Trp emission near 340 nm, owing mainly due to the longer fluorescence lifetimes of the acceptor chromophore. The Dbo emission was not employed in the present analysis.

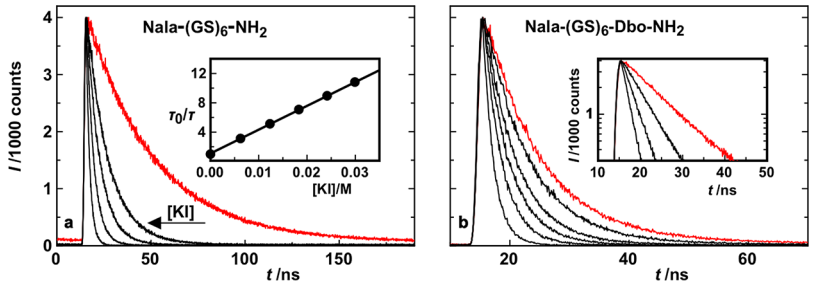

Figure 3. Donor fluorescence decay traces (λ_{exc} = 280 nm, λ_{obs} = 350 nm) for (a) donor-only and (b) donor–acceptor labeled $(GS)_6$ peptide in the absence (red traces) and presence (black traces) of increasing concentrations of KI. The inset in (a) shows the kinetic plot for the determination of the quenching rate constant ($(9 \pm 1) \times 10^9$ M^{-1} s^{-1}), and that in (b) shows the (monoexponential) decays on a logarithmic intensity scale.

enhances FRET significantly, while any movement apart has a comparably smaller effect; this is due to the characteristic R^6 dependence of FRET.[27,66] Consequently, the R_{eff} value determined by FRET in the presence of donor–acceptor diffusion is always shorter than it would be in its absence. However, this also means that variations of the R_{eff} value as they occur when an experimental parameter is systematically varied with the initial distribution remaining unchanged are diagnostic for variations in the contribution of diffusion to FRET, i.e., the FDE.

If the proposition was correct that the FDE can be reduced through donor lifetime reduction by an external quencher, the effective donor–acceptor distance should *increase* with quencher concentration.

Effect of External Quencher on Steady-State and Time-Resolved Fluorescence. We found potassium iodide (KI) to be a highly effective quencher of NAla fluorescence. The required small concentrations (0–30 mM) posed no risks of chain perturbation due to salt effects, which, in the absence of specific binding, is known to occur only at high millimolar or molar concentrations of additives.[67–69]

Upon going from 0 to 30 mM KI, the NAla steady-state fluorescence of the donor-only labeled peptide dropped by more than 1 order of magnitude (factor 12.6, Figure 2a). In the time-resolved measurements, the lifetime of the donor in the donor-only labeled peptide decreased from 35.8 ns (Figure 3a, red trace) to 3.31 ns (lowest black trace). The KI quenching rate constant obtained from the corresponding Stern–Volmer or kinetic plots (insets in Figures 2a and 3a) revealed iodide as a diffusion-controlled quencher of donor fluorescence. The effect of external quencher on the steady-state- and time-resolved-fluorescence emission from the donor in the donor–acceptor labeled peptide (Figure 2b and 3b) was relatively smaller (e.g., from 10.3 to 2.87 ns) due to the intrinsically shorter fluorescence lifetimes in the presence of FRET.

All donor emission decay traces followed monoexponential decay kinetics. This was expected for the donor-only peptide as NAla was specifically chosen for its simple monoexponential decay kinetics, but it was surprising for the double-labeled peptide. As the FRET rate is distance dependent, the kinetics are always expected to be multiexponential in the absence of mutual donor–acceptor diffusion (eq 11). Thus, the observed monoexponentiality of the kinetics provided a first hint for fast diffusion: Short-distance chains (i.e., those with a short donor–acceptor or end-to-end separation) are deactivated faster than long-distance chains but they are replenished sufficiently fast, such that the excited-state distribution decreases in height but retains its shape. A time-invariant shape of the distribution means that the entire excited-state ensemble decays with a single observed rate constant even if the individual chain conformations decay with individual distance-dependent "local" rate constants $k_T(r)$.[70]

The Apparent Donor–Acceptor Distance Is Independent of External Quenching. To evaluate the apparent donor–acceptor distance, R_{eff}, at each KI concentration, the Förster radius was determined at each quencher concentration, because it depends (and decreases) with the donor fluorescence quantum yield, Φ_D (eq 3). Going from 0 to 30 mM KI, the quantum yield of NAla measured for NAla-$(GS)_6$ and calculated from the steady-state-fluorescence spectra relative to *N*-acetyltryptophanamide as reference (Φ = 0.14, pH 7.0)[39,50,51] decreased from 14 to 1.1% (Figure 4a), affecting a marked decrease in the Förster radius from 9.8 to 6.3 Å (Figure 4b). Note that the overlap integral, *J*, and the refractive index, *n*,

dx.doi.org/10.1021/jp310381f | J. Phys. Chem. B 2013, 117, 185–198

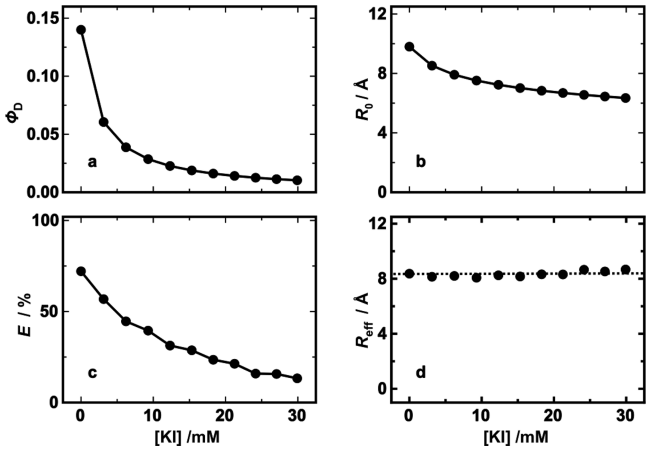

Figure 4. (a) Donor quantum yield, (b) Förster radius, (c) ETE, and (d) recovered effective donor−acceptor distance plotted against KI concentration for the NAla-$(GS)_6$-Dbo peptide. (d) The dotted horizontal line at 8.3 Å is drawn at the average of the R_{eff} values.

were independent of the low millimolar KI concentration. The ETE values were subsequently determined from the donor-only and donor−acceptor fluorescence decay kinetics (Figure 3) via eq 6 by using the R_{DA} values from eq 5 (Figure 4c). It is important to note that the fluorescence decays of the donor−acceptor labeled peptide remained monoexponential even in the presence of quencher.

The presence of quencher—to our great astonishment as experimentalists—led not to the slightest modification of the recovered effective donor−acceptor distance. It remained at about 8.3 Å (Figure 4d), regardless of the dramatic shortening in donor lifetime by more than 1 order of magnitude, which should intuitively limit "the time for diffusion" and therefore the probability to enhance FRET by diffusion, which in turn should result in longer effective distances as quencher is added. The experimental choices we made had permitted highly precise measurements; the conclusion is inevitable that an external quencher that reduces the donor lifetime does not reduce the impact of diffusion on FRET. If it would, the R_{eff} value should have increased as quencher was added. To support this last assumption, we carried out two control experiments, again inspired by the random-walk equation (eq 1), which suggests that the effective distance should increase with either a decreasing diffusion coefficient or with a shorter-lived donor.

Diffusion-Enhanced FRET in Dependence on Solvent Viscosity and Donor Lifetime. Gly−Ser peptides including $(GS)_6$ display no internal friction;[60,71] their end-to-end diffusion coefficient is expected to be directly proportional to the reciprocal macroscopic solvent viscosity, $D \propto \eta^{-1}$, given that the macroviscosity and the relevant microviscosity of the solutions are identical.[38,46,60,61] To demonstrate the influence of viscosity, we measured the R_{eff} value for NAla-$(GS)_6$-Dbo in water and in 90% (v/v) ethylene glycol, that is, at a 12.7-fold higher viscosity;[46,47] we observed an increase in R_{eff} value by about 3 Å (Figure 5, Table 1). This increase is as expected when diffusion is limited. Of course, it cannot be simply ruled out that substituting water for an aqueous solution of a viscogen modifies not only chain dynamics but also structure, as we previously observed for polyproline peptides dissolved in propylene glycol.[41,42]

Conversely, to demonstrate the influence of the donor lifetime, we compared NAla-$(GS)_6$-Dbo and FTrp-$(GS)_6$-Dbo.

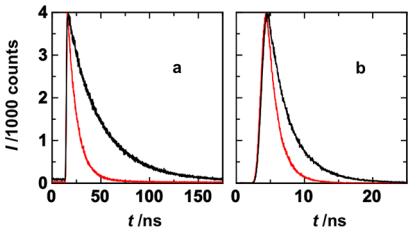

Figure 5. Donor fluorescence decay traces of (a) NAla-$(GS)_6$-Dbo (λ_{exc} = 280 nm, λ_{obs} = 350 nm) and (b) FTrp-$(GS)_6$-Dbo (λ_{exc} = 280 nm, λ_{obs} = 350 nm) in water (red traces) and in 90% (v/v) ethylene glycol (black traces).

The isosteric donors, NAla and FTrp, are not expected to have a significantly different influence on the structure and dynamics of the common Donor-$(GS)_6$-Dbo peptide chain. When the lifetime was decreased about 18-fold, from 35.8 ns for NAla to 1.96 ns for FTrp, R_{eff} increased again by about 3 Å. Thus, the variation of both parameters by more than 1 order of magnitude, donor lifetime and diffusion coefficient (viscosity), yielded the expected result: The apparent distance increased significantly (by ca. 3 Å).[72]

This result contradicted the absence of an observed effect of quencher: If the shortening of the fluorescence lifetime by more than 1 order of magnitude (from NAla to FTrp) has a sizable effect if different donors are utilized, why is the same effect not detectable if the fluorescence lifetime of NAla itself is varied by more than 1 order of magnitude through addition of quencher? To answer this question, we decided to couple the tools of elementary FRET analysis to simulations based on the Haas−Steinberg equation.

Diffusion-Enhanced FRET Studied by Coupling Elementary and Haas−Steinberg Analysis. With one notable exception,[37] the FDE has not been studied on the level of elementary FRET analysis before. To understand, corroborate, and generalize the experimental results, we needed to link the traditional evaluation of FRET measurements to the more complex analysis based on the HSE (eq 9).[1,2,27,29,73] We did that with three questions in mind: (i) Does the HSE predict a symmetrical dependence of the FDE on the donor lifetime and the donor−acceptor diffusion coefficient as demanded by eq 1? (ii) Which donor lifetime should be used in eq 1 if it is not the experimental one? (iii) Can the HSE explain the inefficiency of external quenchers in reducing the FDE?

The HSE relates the rate of donor deactivation to the sum of three terms accounting for the donor decay in the absence of FRET, for the donor decay caused by FRET, and for diffusion.

$$\frac{\partial N^*(r,t)}{\partial t} = -k_D N^*(r,t) - k_D \frac{R_0^6}{r^6} N^*(r,t) + \frac{\partial}{\partial r}\left(N_0^*(r) D \frac{\partial (N^*(r,t)/N_0^*(r))}{\partial r} \right) \quad (9)$$

A visual illustration of the HSE, first derived in ref 27, is given in Figure 6, which shows an exemplary distance distribution, $N_0^*(r)$ or $N_0^*(r,t=0)$, instantly after short-pulse donor excitation. Because the probability of donor excitation should be independent of the conformation of the peptide chain (and because there is no indication for exciplexes between the selected donors and the acceptor), the initial distance probability distribution of excited states, $N_0^*(r)$, normalized to $\int N_0^*(r)\, dr = 1$, is identical to the probability

dx.doi.org/10.1021/jp310381f | J. Phys. Chem. B 2013, 117, 185−198

Table 1. FRET Analysis of Donor-$(GS)_6$-Dbo Peptides

donor	solvent	Φ_D	τ_D/ns	τ_0/ns	τ_{DA}/ns	R_0/Å	E^a/%	$R_{eff}{}^b$/Å
NAla	water	0.14	35.8	256	10.3	9.8	70.5	8.4
	ethylene glycol[c]	0.20	51.9	260	33.1	10.2	36.2	11.2
FTrp	water	0.10	1.96	19.6	1.50	9.6	24.8	11.7
	ethylene glycol[c]	0.23	3.68	16.0	2.96[d]	11.1	19.7	14.1

[a]Energy transfer efficiency from time-resolved-fluorescence measurements (eq 6). [b]Effective distance determined from E and R_0 (cf. eq 5). [c]With 90% (v/v) ethylene glycol, pH 5.0, 25 °C. [d]τ_{DA} is an amplitude-weighted lifetime obtained from $\tau_{DA} = \alpha_1\tau_1 + \alpha_2\tau_2$ = 0.62·2.26 ns + 0.38·4.11 ns.

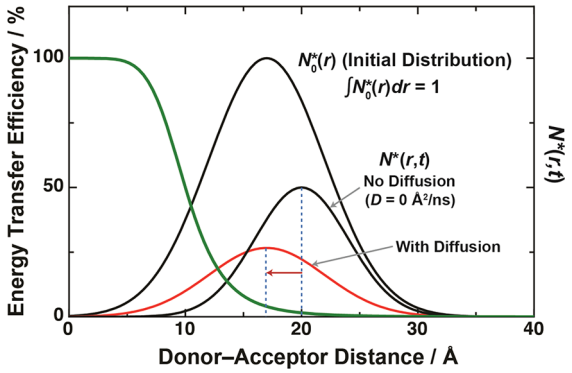

Figure 6. Diffusion-enhanced FRET. The initial (t = 0, solid black line) distance distribution of chains with excited donor is identical to the ground-state probability distance distribution in the equilibrium chain ensemble, $N_0{}^*(r) = N^*(r,t{=}0) = p(r)$ with $\int p(r)\,dr = 1$. After excitation, chains with proximate donor and acceptor are rapidly deactivated and the distribution is down-sized and continuously shifted to larger distances (dotted line). However, if the labeled sites can approach each other by mutual diffusion, short-distance chains are continuously replenished (red line) such that the observed ETE, E_{obs}, is raised. The green line marks the local ETE, $E(r)$, for a particular distance.

distribution in the ground-state equilibrium ensemble of chains, i.e., $N_0{}^*(r) = p(r)$ (Figure 6, solid black line). Subsequently, more chains with a short donor–acceptor distance undergo FRET than long-distance chains, such that the distribution $N^*(r,t)$, is shifted toward longer distances (Figure 6, dotted line). Mutual donor–acceptor motion counteracts this trend by constantly replenishing short-distance chains (Figure 6, red line). From the HSE, the donor decay kinetics can be generated for any distribution, diffusion coefficient, and donor lifetime.

How can we quantify the FDE? Central to traditional FRET analysis is the ETE as the fraction of donor deactivation events caused by FRET. The ETE can be viewed as being composed of a contribution, E_0, from the initial distance distribution as it would develop in the absence of diffusion and of a contribution from diffusion that yields the additional efficiency, ΔE_{FDE} (eq 10).

$$E_{obs} = E_0 + \Delta E_{FDE} \tag{10}$$

To obtain these quantities from the HSE, one needs to generate and evaluate the following kinetic traces of donor fluorescence intensity (Figure 7 a).

(i) The donor decay in the absence of FRET, in the donor-only peptide (Figure 7 a, black dashed curve): The associated fluorescence intensity, $I_D(t)$, follows eq 11. The emitted fluorescence is given by the area under the curve, A_D. The initial intensity is set to 100%, such that the values of the area and donor lifetime become identical: $A_D = k_D{}^{-1} = \tau_D$.

$$I_D(t) = I_0 \exp(-k_D t) \tag{11}$$

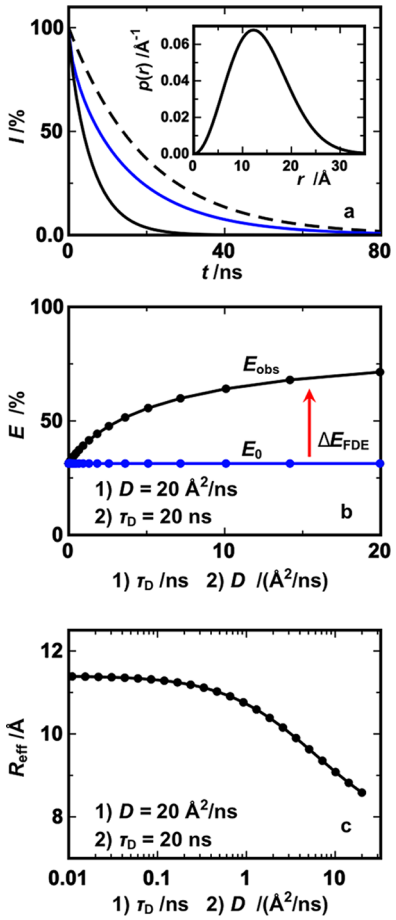

Figure 7. HSE simulations (at constant donor quantum yield). (a) Simulated decay traces of donor fluorescence in the donor-only peptide (dashed line), the donor–acceptor peptide in the absence of diffusion, D = 0 (blue), and the donor–acceptor peptide in the presence of diffusion with D set to 20 Å²/ns (black). Further parameters were τ_{DA} = 20 ns, R_0 = 10 Å, and the minimal and maximal distances of approach set to 4 and 50 Å, respectively. The areas under the curves were obtained by numerical integration and used to determine the ETE values. Inset: The initial (equilibrium) probability density distribution in an ideal Gaussian chain (eq 14) with $(\langle r^2\rangle)^{1/2}$ set to 15 Å. (b) (1) The observed ETE, E_{obs} (black), and the ETE in the absence of diffusion, E_0 (blue) were plotted against the donor lifetime, while D was kept fixed at 20 Å²/ns. (2) E_{obs} and E_0 were plotted against D while the lifetime was kept fixed at 20 ns. The ETE courses in both simulations coincide. (c) The effective donor–acceptor distance calculated from E_{obs} (eq 5) plotted (1) against the donor lifetime when the diffusion coefficient was fixed at 20 Å²/ns and (2) against the diffusion coefficient when the donor lifetime was set to 20 ns. Both courses coincide.

(ii) The donor decay in the presence of FRET, in the donor–acceptor peptide, but in the absence of diffusion: Its intensity, I_{DA0}, is described by a closed expression (eq 12),

dx.doi.org/10.1021/jp310381f | J. Phys. Chem. B 2013, 117, 185–198

where $p(r) = N_0^*(r)$. Equation 12 is a consequence of the relations $k_{DA}(r) = k_D + k_F(r)$ and $k_F(r) = k_D(R_0/r)^6$ (eq 2). An identical decay can be simulated by setting the diffusion coefficient in the HSE to zero. The area under the curve, A_{DA0}, measures the fluorescence emitted in the absence of diffusion.

$$I_{DA0}(t) = I_0 \int \exp(-k_D t - k_D(R_0/r)^6 t)\, p(r)\, dr \tag{12}$$

(iii) The donor decay in the presence of FRET and diffusion as generated through the HSE: With the distribution $N^*(r,t)$ being determined, the decay follows eq 13 and yields the fluorescence emitted in the presence of diffusion, A_{DAD}.

$$I_{DA}(t) = I_0 \int N^*(r, t)\, dr \tag{13}$$

The efficiencies E_{obs}, E_0, and ΔE_{FDE} are then determined from the simulated areas via $E_{obs} = (A_D - A_{DAD})/A_D$, $E_0 = (A_D - A_{DA0})/A_D$, and $\Delta E_{FDE} = (A_{DA0} - A_{DAD})/A_D$ (cf. eq 7).

To test whether E_{obs} and ΔE_{FDE} depend symmetrically on donor lifetime and diffusion coefficient, we assumed a constant quantum yield and ran two series of simulations. In the first series, the diffusion coefficient was kept fixed at 20 Å^2/ns and the donor lifetime was varied from 0.1 to 20 ns to cover a representative range.[54,65] In the second series, the donor lifetime was held constant at 20 ns and the diffusion coefficient was varied from 0.1 and 20 Å^2/ns, a range which encompasses published diffusion coefficients.[1,2,27,74−76] In the case of a symmetrical dependence, plots of E_{obs} versus lifetime and versus diffusion coefficient would coincide. The HSE simulations used the model of an ideal Gaussian chain for the distribution (eq 14) with a root-mean-square distance of 15 Å (Figure 4a, inset). In subsequent controls, two-parameter distributions were also employed: In the wormlike chain model (eq 15),[77] the parameters l_p and l_c are the persistence and contour length of the chain; in the widely used skewed Gaussian distribution (eq 16) a and b determine the width and position of the distribution, whereas c is determined from the normalization condition.

$$p(r) = 4\pi r^2 \left(\frac{3}{2\pi\langle r^2\rangle}\right)^{3/2} \exp\left(-\frac{3}{2}\frac{r^2}{\langle r^2\rangle}\right) \tag{14}$$

$$p(r) = \frac{4\pi r^2 N}{l_c^2(1 - (r/l_c)^2)^{9/2}} \exp\left(\frac{-3l_c}{4l_p((1 - (r/l_c)^2)^2}\right) \tag{15}$$

$$p(r) = \pi r^2 c \exp(-a(r - b)^2) \tag{16}$$

Indeed, the ETEs, E_{obs}, and ΔE_{FDE} ($=E_{obs} - E_0$) grew in an identical fashion with the diffusion coefficient as well as with the donor lifetime (Figure 7b). Thus, the HSE predicts the diffusion enhancement to depend symmetrically on diffusion coefficient and donor lifetime, that is, to be a function of their product. This symmetry depended neither on the choice of the distance-distribution model (eqs 14−16) nor on the specific parameter choices. The results also confirmed that E_0 was suitably defined and robustly reproduced by the programmed software: It depends neither on the donor lifetime nor on the diffusion coefficient but was constant throughout the simulations (Figure 7b, blue trace). However, does E_0 really measure the information from the equilibrium distance distribution, even under diffusion? This is certainly not the case as this piece of information is gradually lost with increasing diffusion. Later we will introduce a more suitable parameter, fully within the spirit of traditional FRET analysis.

In the two simulation series, the effective distance grew with a decreasing diffusion coefficient in the same manner as with a decreasing donor lifetime (Figure 7c), which confirms that R_{eff} reflects the FDE. Throughout the simulations, the Förster distance was held constant at 10.0 Å. As R_0 depends on the donor quantum yield (eq 2), the simulations cover only the case of a *constant quantum yield*, that is, of intrinsic donor-lifetime variations as they occur for two chromophores with different fluorescence lifetimes but the same quantum yield. Qualitatively, the simulations agree with the intuitive expectation and the experimental results in that both, a donor-lifetime reduction and a raised solvent viscosity, lead to an increased effective distance. We had to explain why the same does not hold when the donor lifetime is reduced by addition of an external quencher. In attempting to do so, it is important to realize that an external quencher reduces the fluorescence lifetime to the same extent that it reduces the fluorescence quantum yield.

The Radiative Donor Lifetime Dominates the FDE. The measured donor lifetime in the donor-only peptide, τ_D, is not simply the lifetime that controls the FDE. The lifetime τ_D, or its reciprocal quantity, k_D, can be dissected into two components (eq 17): The radiative decay rate k_{rad} is the rate of donor emission when the donor quantum yield, Φ_D, equals unity, that is, when each photon absorbed by the donor leads to one being emitted. The rate k_{nrad} captures nonradiative decay processes including quenching by a coagent. Addition of an external quencher raises only k_{nrad} and reduces, by that, the donor quantum yield defined by eq 18. What the experiments suggest, therefore, is that the nonradiative decay rate has no or little influence on the FDE and that it is the radiative lifetime, $\tau_0 = k_{rad}^{-1}$, that has to be changed to alter the FDE and the effective distance. In the context of FRET, it is, in fact, well-known and has often been emphasized that k_T only depends on τ_0,[22,78] but in the context of FDE, where a correlation between FDE and τ_D seems intuitive, this conclusion is more difficult to reach.

$$k_D = k_{rad} + k_{nrad} \tag{17}$$

$$\Phi_D = k_{rad}/(k_{rad} + k_{nrad}) \tag{18}$$

$$k_{rad} = \Phi_D k_D \tag{19}$$

$$\tau_D = \Phi_D \tau_0 \tag{20}$$

An impact of the nonradiative decay rate or of the quantum yield on the FDE could be expected if the rate of FRET at a specific distance would depend on the quantum yield. At first glance, this appears to be the case because k_T depends on k_D (eq 2, $k_T = k_D(R_0/R_{DA})^6$), which itself depends on Φ_D (cf. eq 19, $k_D = k_{rad}/\Phi_D$). Yet, according to the fundamental but less frequently employed equation that Förster derived (eq 21),[78] the distance-dependent FRET rate is independent of Φ_D. In the next step, we needed to confirm by HSE simulations that the same held for the diffusion-enhanced FRET rate. At first, we determined what had to be done differently in this set of simulations than in the previous one (Figure 7): Collecting all constants in eq 21 into one, $cJ\kappa^2/n^4 = R_F^6$, yields eq 22.

$$k_T = (cJ\kappa^2/n^4)(k_{rad}/R_{DA}^6) \tag{21}$$

$$k_T = k_{rad}R_F^6/R_{DA}^6 \tag{22}$$

dx.doi.org/10.1021/jp310381f | J. Phys. Chem. B 2013, 117, 185−198

Thus, R_F is the donor−acceptor distance ($R_{DA} = R_F$) at which the donor emits a photon with an equal probability as it transfers its excitation energy to the acceptor, $k_T = k_{rad}$. The distance R_F equals the Förster radius only at a quantum yield of unity. In contrast, the Förster radius R_0 is the distance at which donor deactivation by FRET is as likely as donor deactivation by all alternative processes including photon emission but also collision-induced quenching. The condition that $k_T = k_D$ when $R_{DA} = R_0$ allows rewriting eq 21 as the familiar eq 2, $k_T = k_D R_0^6/R_{DA}^6$. By using eq 19, we can rewrite eq 22 as $k_T = \Phi_D k_D R_F^6/R_{DA}^6$ to obtain the relationship between R_0 and R_F (eq 23). It follows that, although both the Förster radius and the measured donor lifetime depend on the quantum yield, k_T does not because the product $k_D R_0^6$ in eq 2 remains constant as the quantum yield is changed: $k_D R_0^6 = k_{rad}\Phi_D^{-1}\Phi_D R_F^6 = k_{rad} R_F^6$ (eq 24; cf. eqs 19 and 23).

$$R_0^6 = \Phi_D R_F^6 \tag{23}$$

$$k_D R_0^6 = k_{rad} R_F^6 \tag{24}$$

In the foregoing series of simulations, we left the Förster radius unchanged while we varied the lifetime. Thus, in essence, we varied the radiative lifetime and learned that the FRET diffusion enhancement depends symmetrically on the *radiative* lifetime and the diffusion coefficient. However, when we simulate the effect of external quenching by changing the quantum yield and, by that, the donor lifetime, we must keep the product $k_D R_0^6$ constant (eq 24). The HSE can be appropriately rewritten for this set of simulations (eq 25).

$$\frac{\partial N^*(r,t)}{\partial t} = -\frac{k_{rad}}{\Phi_D}N^*(r,t) - \frac{k_{rad}R_F^6}{r^6}N^*(r,t) + \frac{\partial}{\partial r}\left(N_0^*(r)D\,\frac{\partial N^*(r,t)/N_0^*(r)}{\partial r}\right) \tag{25}$$

HSE and Traditional FRET Analysis of the FDE Quantum-Yield Dependence. We set the radiative donor lifetime, $\tau_0 = k_{rad}^{-1}$, to 250 ns and the radiative Förster radius, R_F, to 14 Å to mimic the radiative lifetime of NAla and the radiative Förster radius of the NAla/Dbo donor/acceptor pair (13.7 Å). The quantum yield was varied from 1 to 0.01, thereby mimicking a donor lifetime variation ($\tau_D = k_D^{-1}$) from 250 to 2.5 ns. Further simulation details are described in the legend of Figure 8.

For the selected distance distribution (Figure 8a, black line), a donor−acceptor pair with a Förster radius of 14 Å would be a proper experimental choice. In the absence of diffusion (Figure 8a, blue dotted lines), the probability density shifts significantly with time, as expected. In contrast, in the presence of diffusion, the initial probability distribution rapidly develops into a stationary distribution. This is seen when the distributions $N^*(r,t)$ obtained after 5, 100, and 200 ns are normalized and compared. The obtained $p(r,t)$ profiles coincide well (Figure 8a, red line). It is remarkable how fast the stationary state is reached and how closely the ground-state equilibrium and the stationary excited-state distribution resemble each other. When the distance at the distribution peak is plotted against time, a stable plateau is reached after about 2 ns (Figure 8b). The same courses are obtained for quantum yields of 1.0 and 0.1, as only quenching by FRET is distance-dependent and able to alter the shape of the distribution. When diffusion is absent, a plateau is never reached (Figure 8c), and the distribution continues to shift to higher distances.

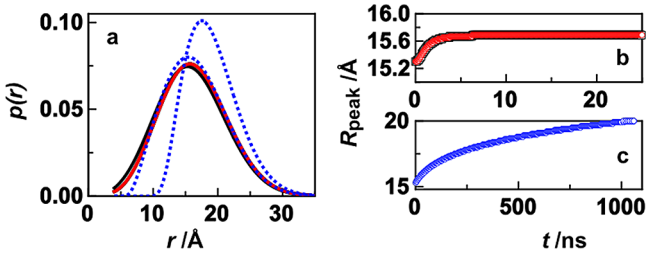

Figure 8. HSE results for τ_0 = 250 ns, R_F = 14 Å, and a skewed Gaussian distance distribution (eq 16) with a = 0.0123 Å^{-2} and b = 10 Å. (a) Black line: equilibrium probability distribution. Red line: probability distance distribution with diffusion (D = 20 Å^2/ns) after 5, 100, and 200 ns. The curves virtually coincide. Also shown are the probability distance distributions in the absence of diffusion after 5 ns (left-hand dotted blue line) and 100 ns (right-hand line). Note that, due to the normalization utilized in this graph ($\int p(r)\,dr = 1$), the narrower distribution is higher. (b) Distance of the distribution peak in the presence of diffusion (D = 20 Å^2/ns) plotted against time for Φ_D = 1 (red) and 0.1 (black). The courses coincide. (c) Time course of the distribution-peak distance in the absence of diffusion.

With quenching, i.e., decreasing quantum yield and donor lifetime, the efficiencies, E_{obs} and E_0, decreased and approached zero (Figure 9a), whereas the effective distance calculated from

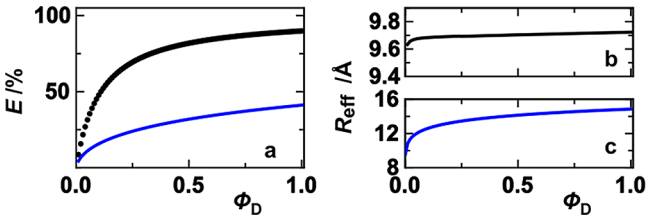

Figure 9. (a) Observed ETE, E_{obs} (black), in the presence of diffusion (D = 20 Å^2/ns), and ETE in the absence of diffusion, E_0 (blue), plotted against the quantum yield. Quantum-yield dependence of the effective distance (b) in the presence of diffusion (D = 20 Å^2/ns) and (c) in the absence of diffusion (blue), as calculated from (b) E_{obs} and (c) E_0 (cf. eq 5), and $R_0 = \Phi_D^{1/6}R_F$.

E_{obs} (cf. eq 5) and from R_0 ($R_0 = \Phi_D^{1/6}R_F$; cf. eq 23) remained virtually constant (Figure 9b). Only at very small values of the quantum yield was a minimal decrease observed (Figure 9b). Recall that a successful minimization of the FRET diffusion enhancement should result, according to the original intuitive anticipation, in an increase and not in a decrease of the effective distance. Thus, both experiment and simulation indicate that an external quencher cannot increase the effective distance in contrast to the two other strategies of FDE reduction that we tested—raising the viscosity and shortening the radiative lifetime by the choice of a different donor.

It is important to realize the consequences of how strongly the effective distance in the absence of diffusion decreased with decreasing quantum yield (Figure 9c, blue line). A multitude of studies have been aimed at extracting effective distances and distance trends from FRET ensemble measurements,[10,14,40,79,80] but none has taken into account that the quantum yield does not merely alter R_0, but that it indeed changes the measured effective distance. This conclusion reaches far: For FRET to yield reliable information on distance trends in an experimental series of polydisperse polymers or

dx.doi.org/10.1021/jp310381f | J. Phys. Chem. B 2013, 117, 185−198

biopolymers, particularly in the absence of diffusion, a constant quantum yield needs to be maintained, or corrections according to those outlined herein would need to be made. Note that the donor quantum yield can easily increase or decrease in an experiment when, for instance, a protein folds,[10,14] when the temperature is varied, or when a coadditive is added.[40] The R_{eff} trend might then be interpreted as a shortening of the monitored distance where, in reality, none is taking place. Note that, in reaching this result, we do not exclusively rely on HSE simulations; we obtain an identical quantum-yield dependence of the effective distance from a closed analytic expression derived in the Supporting Information.

$$R_{eff} = \Phi_D^{1/6} R_F \, (1/(1 - \int p(r) r^6/(r^6 + \Phi_D R_F^6)\, dr) - 1)^{1/6} \quad (26)$$

The most appropriate perspective to understand the results on not merely the mathematical but also the physical level is to analyze them in terms of the effective FRET rate constants, k_{FRET} and k_{FRET0}, in the presence and absence of diffusion. Earlier, we demonstrated that the Förster rate at a specific distance, $k_T(r)$, is independent of the quantum yield. However, the effective FRET rate obtained by measurement is defined through E_{obs} ($k_{FRET} = k_D(1/E_{obs} - 1)^{-1}$; cf. eq 4); that is, it accounts for FRET at all distances accessible to the chain. It now turns out that the effective k_{FRET} value for the entire distribution (which is experimentally accessible) *does vary with the quantum yield*, not because the microscopic FRET rates (at a fixed distance) depend on the quantum yield, but because the quantum yield (quenching) dictates which distances contribute more highly to the effective FRET rate. This variation is more pronounced in the absence of diffusion.

Note Figure 10a. k_{FRET} remains almost constant with the quantum yield in the presence of diffusion. That it shares this behavior with the effective distance (cf. Figure 9b) is expected as the equation $k_{FRET} = k_D(R_0/R_{eff})^6$ holds for the effective parameters. In the absence of diffusion, for k_{FRET0}, it is again possible to obtain an analytic expression for the quantum-yield dependence (eq 27) that can be derived, for instance, from the fluorescence of the donor–acceptor peptide as given by the area under the donor–acceptor decay, $A_{DA0} = \int\int \exp(-(k_D + k_{FRET})t)\; p(r)\; dr\; dt$ (cf. eqs 5 and 14). Two alternative derivations are given in the Supporting Information.

$$k_{FRET0} = k_{rad}\Phi_D^{-1}((\int p(r)/(1 + \Phi_D R_F^6/r^6)\, dr)^{-1} - 1) \quad (27)$$

Thus, the dependence of k_{FRET} on the quantum yield is strongest in the absence of diffusion and vanishes with increasing diffusion. In the limit of very fast diffusion, the equilibrium or initial distance probability distribution is maintained at all times, the observed kinetic traces are monoexponential, and the effective FRET rate is equal to the distance average of the Förster rate, k_T.[81] One has $k_{FRET} = \langle k_T \rangle = \int k_T(r)\; p(r)\; dr = \int k_D(R_0^6/r^6)\; p(r)\; dr = k_{rad}R_F^6\langle r^{-6}\rangle$, i.e., an obvious independence of the quantum yield. We are close to this case in both experiments—where we obtained monoexponential kinetics for NAla-$(GS)_6$-Dbo and the simulations (Figure 8a)—where a stationary distribution, hardly distinguishable from the equilibrium distribution, is quickly attained. More details are discussed in the Supporting Information.

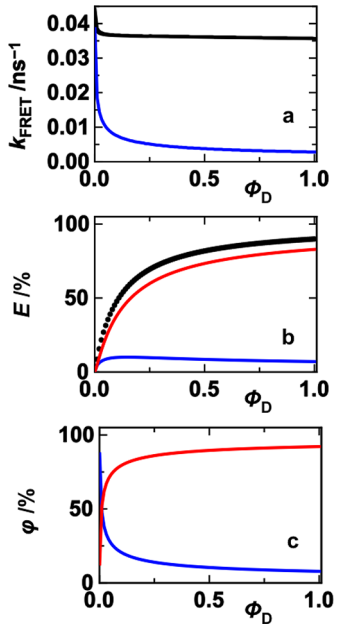

Figure 10. (a) Observed FRET rate, k_{FRET} (black line), calculated from E_{obs} (cf. eq 4), and FRET rate for the static distribution, k_{FRET0} (blue), calculated from E_0 (and $R_0 = \Phi_D^{1/6}R_F$) plotted against the quantum yield. (b) E_{obs} (black line), E_{EQ}, the fraction of donor deactivation events caused by FRET due to the equilibrium distance distribution (blue), and E_M, the fraction of deactivation events caused by FRET due to donor–acceptor motion (red), plotted against the donor quantum yield. (c) Fraction of FRET events, $\varphi_0 = E_{EQ}/E_{obs} = k_{FRET0}/k_{FRET}$, caused by the initial distance distribution (blue) and the fraction of FRET events, $\varphi_M = E_M/E_{obs} = 1 - \varphi_{EQ}$, caused by donor–acceptor motion (red) plotted against the donor quantum yield. Simulations in the presence of diffusion were performed with $D = 20$ Å^2/ns.

It is obvious that the decomposition of the ETE by $E_{obs} = E_0 + \Delta E_{FDE}$ cannot help to quantify the FDE under quantum-yield variation. The ETE in the presence and absence of diffusion decreases strongly as the quantum yield decreases (Figure 9a) while with diffusion the effective distance and FRET rate are virtually constant (Figures 9b and 10a). To apprehend when and why a quantum-yield dependence of the effective parameters can occur and to quantify the information that a time-resolved FRET experiment can yield on the equilibrium distance distribution and on diffusion, we have to use the effective FRET rates, k_{FRET} and k_{FRET0}, to decompose the ETE.

The ETE is the fraction of donor deactivation events caused by FRET, $E_{obs} = \Delta N^*_{FRET}/\Delta N^*$ or $E_{obs} = k_{FRET}/(k_{FRET} + k_D)$. We are interested in the fraction of donor-deactivation events that can be attributed to FRET from the initial (or the equilibrium) distance distribution, E_{EQ}, as well as to FRET from diffusional motion, E_M (read "E_{Motion}"). We are specifically interested in the *fraction of FRET events* that can be attributed to the equilibrium distribution, φ_{EQ}, and to diffusion, φ_M. With k_{FRET} and k_{FRET0} obtained from E_{obs} and E_0, we can define and determine these quantities (eqs 28–32).

$$E_{obs} = E_{EQ} + E_M \quad (28)$$

$$E_{EQ} = k_{FRET0}/(k_{FRET} + k_D) \quad (29)$$

$$E_M = (k_{FRET} - k_{FRET0})/(k_{FRET} + k_D) \quad (30)$$

dx.doi.org/10.1021/jp310381f | J. Phys. Chem. B 2013, 117, 185–198

$$\varphi_{EQ} = k_{FRET0}/k_{FRET} \quad (31)$$

$$\varphi_{M} = (k_{FRET} - k_{FRET0})/k_{FRET} \quad (32)$$

It follows that $\varphi_{EQ} = E_{EQ}/E_{obs}$, $\varphi_{M} = E_{M}/E_{obs}$, and $\varphi_{EQ} + \varphi_{M} = 1$.

As Figure 10b shows, the diffusion contribution, E_M, contributes the overwhelming part to the ETE and decreases in parallel to it while the quantum yield decreases. The FRET contribution of the equilibrium distribution, E_{EQ}, stays small and is much smaller than the ETE in the absence of diffusion, E_0 (Figure 9a), despite a Förster radius of 14 Å that would appear to be an excellent experimental choice as it is close to the average distance of the distribution (Figure 8a). As E_{EQ} mirrors the absolute signal or information from the equilibrium distribution, it clearly transpires that suppressing diffusion might often be the only means to access the sought-after equilibrium distances. However, adding an external quencher, to dwell on this once more, leads only to a loss of information.

When the quantum yield is small, the activated donor has little chance to emit a photon and to contribute to the measured fluorescence signal. However, if the distance to the acceptor is too large, the donor's chance is also small to transfer its energy to the acceptor and to contribute to the measured difference between the emission of the donor–acceptor peptide and that of the donor-only peptide. Thus, the lower the quantum yield, the more chains of the equilibrium distribution become literally invisible; the higher the distance, the more chains are simply not monitored as if they were not present in the first place. This explains why, in the absence of diffusion, the effective FRET rate increases and the effective distance decreases with decreasing quantum yield, with both giving the impression of shorter distances present in the equilibrium distribution than is in reality the case.

At a very small quantum yield, it is only at a very short distance where the FRET rate is sufficiently high to compete with the rate of external quenching. However, when the distance is so short, FRET occurs before the donor and acceptor can considerably change their distance. This explains the observed variation of φ_{EQ} and φ_{M} (Figure 10c). The fraction of FRET events caused by the equilibrium distribution, φ_{EQ}, tends to go toward 100% as the quantum yield approaches zero. In this extreme, all FRET events that still take place have to be attributed to the short-distance tail of the initial ($t = 0$) distribution. The fraction of FRET events due to diffusion, φ_{M}, decreases first very weakly with decreasing quantum yield to drop dramatically at very low values ($\varphi_{EQ} + \varphi_{M} = 1$).

Are there any circumstances under which FRET measurements at a reduced quantum yield (high quencher concentration) can add new information to that obtained from a measurement at a high quantum yield? For time-resolved-fluorescence measurements, this is likely not the case. The kinetic trace of the donor–acceptor peptide starts with an initial steep decline that is caused by the short-distance tail of the distribution, where FRET is fastest. With increasing quencher concentration, any "later" signal from the bulk of the distribution is gradually eliminated. Thus, quantum-yield variation by adding an external quencher cannot add new information but is merely equivalent to evaluating only the beginnings of the kinetic traces obtained at a high quantum yield. A global analysis of the decay traces obtained at successively increasing quencher concentration can only distort the result as it puts an increasing weight on the information that stems from the short-distance parts of the equilibrium distribution. This approach is therefore inferior to simply repeating the measurements at the highest quantum yield to so benefit from an increased signal-to-noise ratio of the averaged kinetics. The target to modulate the FDE of the whole equilibrium distribution, which is a precondition for a meaningful global analysis, cannot be attained through an external quencher. Of course, quantum-yield variations can be of benefit for other spectroscopic methods aimed at characterizing the dynamics of a polymer chain, e.g., when they are based on excimer formation instead of FRET.[82]

DISCUSSION

Diffusion-Enhanced FRET Is Independent of the Donor Quantum Yield. The random-walk equation captures the intuition that the impact of internal chain motions on FRET could be minimized by minimizing the donor lifetime through an external quencher. Lakowicz and co-workers predicted that "...collisional quenching can be used to decrease the decay time of the donor. Under these conditions of shortened donor lifetime, there is less time for diffusion, and the data contain more information on the initial $t = 0$ distance distribution."[34] This would indeed be the case if the donor–acceptor displacement that can occur during the donor lifetime, τ_D ($\Delta R_{rms} = (6D\tau_D)^{1/2}$, eq 1), would be a proper measure of the FRET diffusion enhancement. As it is otherwise hard to escape from this thinking pattern—similar reasoning has found its way into a fundamental textbook[54]—we decided to demonstrate its incorrectness not merely by theoretical arguments but also by experiment and simulation. For further discussion, however, we formulate a simple analogy that can convey why external quenching can hardly affect the FDE: The effect of adding a quencher to the measurement solutions of the donor-only and donor–acceptor labeled peptides is identical to the effect that it would have when the solutions would be continuously diluted during measurement. The donor deactivated by a quencher or removed by dilution neither can emit a photon (to so contribute to the measured fluorescence signal) nor can it transfer its excitation energy to the acceptor (to so contribute to the signal difference between single- and double-labeled peptides). The quencher reduces the observed ETE but affects the FDE defined by $\varphi_{M} = E_{M}/E_{obs}$ only weakly and only by eliminating the information from the bulk of the distribution. Reducing the donor lifetime by reducing the donor quantum yield merely compromises the signal-to-noise ratio. At this stage, these conclusions might appear almost self-evident, but they imply surprising and important consequences.

Lakowicz and co-workers studied the dynamics and structure of the chain $(CH_2)_{22}$ labeled by the FRET donor–acceptor pair tryptamine (TMA) and dansyl.[34] The Förster radius decreased from 24.9 Å in the absence to 20.1 Å in the presence of 9.3 mM acrylamide (cf. eq 20). The time-resolved-fluorescence responses of the donor-only and donor–acceptor chains in the absence and presence of quencher were globally fitted to the HSE used with a Gaussian distribution model. The recovered diffusion coefficient (126 Å^2/ns) was about half that of the free probes (264 Å^2/ns), and the average distance and full width at half-maximum were determined to be 18.9 Å and 17.1 Å. Whereas the analysis of the unquenched samples could not yield such a defined set of values, a remarkable resolution enhancement was achieved when the results from the quenched and unquenched samples were simultaneously fitted. This observation was attributed to the lower impact of

dx.doi.org/10.1021/jp310381f | J. Phys. Chem. B 2013, 117, 185–198

diffusion on FRET and to the higher impact of the initial distance distribution in the presence of quencher. As we demonstrated by experiment, by simulation, and by theoretical arguments, this intuitive reasoning could not have been the cause for the observed resolution enhancement: The data in the presence of quencher do not add new information. The problem—expressed as mathematical analogy—remains that two unknowns cannot be determined from a single equation and also not from a multitude of linearly dependent equations that all contain the same information. The apparent resolution enhancement was more likely a consequence of an (unintended) increased weighing of the information from the short-distance parts of the distribution.

The Random-Walk Perspective Revisited and Applied to Global Analysis. In other cases, the conditions for a successful global analysis are only apparently met. In a recent investigation on how the denaturant guanidinium chloride (GdmCl) influences the peptidic chain $(GS)_{16}$, the two donors naphthylalanine (NAla) and pyrene (Py) were alternately used in combination with dansyl as acceptor (Dans).[38] The Förster radii of the pairs are similar (NAla/Dans, 22.3 Å; Py/Dans, 20.5 Å) and the experimental donor lifetimes of Py (226 ns) and NAla (37 ns) seemed to guarantee a much larger FDE in the Py/Dans chain than in the NAla/Dans chain. In the original article, the diffusion coefficient in water was reported as 4 Å^2/ns and the average end-to-end distance was reported as 19 Å.[38] These values were later drastically corrected by 1 order of magnitude to D = 50 Å^2/ns and by a factor of 2 to R_{av} = 38 Å in water and to D = 60 Å^2/ns and R_{av} = 50 Å in the presence of 8 M GdmCl.[61] We base the following considerations on the corrected results.

At the average distance of 38 Å, the probability and rate of FRET are negligibly small in relation to the fluorescence decays (NAla, k_T = 0.0011 ns^{-1}; Py, k_T = 0.00011 ns^{-1}). FRET becomes fast only at distances shorter than R_0 (e.g., $k_{T,NAla}$ (12 Å) = 1.11 ns^{-1}, $k_{T,Py}$ (12 Å) = 0.11 ns^{-1}). In water, the bulk of the equilibrium distance distribution contributes negligibly to the ETE (NAla, $E_0 \sim 4\%$; Py, $E_0 \sim 2\%$; eq 4), and even less at 8 M GdmCl (NAla, $E_0 \sim 1\%$; Py, $E_0 \sim 0.5\%$). If we next apply the corrected random-walk equation[54] (eq 1, $\Delta R_{rms} = (6D\tau_D)^{1/2}$), we obtain the displacement that can occur in the absence of FRET until the donor is deactivated by photon emission or quenching, $\tau_D = (\tau_0^{-1} + \tau_{nrad}^{-1})^{-1}$. The ΔR_{rms} value is 105 Å for NAla and 260 Å for Py. If these values would properly indicate the FDE, Py would indeed lead to a much larger FDE than NAla. However, the Results demonstrate beyond doubt that the FDE does not depend on the quantum yield but only depends on the radiative lifetime. Hence, when we want to use the displacement to quantify the FDE, we have to calculate it from τ_0. The displacements are then 277 Å for NAla ($\Phi_D \sim 0.14$, $\tau_0 \sim$256 ns) and 313 Å for Py ($\Phi_D \sim 0.69$, $\tau_0 \sim$ 328 ns). The radiative lifetimes are similar and, as a consequence, also the displacement values are similar. While the donor lifetimes differ by more than 1 order of magnitude, the displacement values relevant for assessing the FDE differ by merely 18%, a small difference considering the 50% variation in size of the two aromatic donors. The two donor pairs (NAla and Py) have been, in retrospect, only apparently ideal for the intended FRET analysis.

Be this as it may, the similar, very large displacement values (ca. 300 Å) ascertain that donor and acceptor are always able to traverse through regions of negligible FRET probability to reach distances at which FRET becomes fast, i.e., distances shorter than the Förster radii. For a global analysis, this situation is far from ideal, as FRET is almost completely caused by diffusion: φ_M, the fraction of FRET events due to diffusion, approaches 100%, while φ_{EQ} vanishes, no matter whether NAla or Py is used as donor. Such measurements can at best provide a possible lower limit for the dominant distances present in solution and can inform on neither the kind nor the shape of the distribution, certainly not at distances larger than the R_0 value. As becomes obvious from Figure 7c, any variation in the product of τ_0 and D would need to cover at least 2 orders of magnitude difference to cover the regimes of fast diffusion (the region with negative slope in Figure 7c) to negligible diffusion (plateau region). In any case, a reliable delineation of diffusion coefficient and distribution requires at least a minimum of FRET, of information, from the equilibrium distances present in solution. The optimal basis for a global analysis would be measurements where φ_{EQ} varies gradually from 100 to 0%. In a minimalist approach, at least two conditions should be studied: one with φ_{EQ} significantly above and the other with φ_{EQ} significantly below 50%. The NAla/Dans and Py/Dans pairs fall short of this requirement, because φ_{EQ} is virtually zero (φ_M = 100%) for both. We have to ask about ways to realize improved conditions.

Conditions for a Successful Delineation of Polypeptide Structure and Dynamics. A modest FDE, a modest possible displacement, ΔR_{rms}, requires that the equilibrium distance distribution is mainly defined by distances at which FRET is fast: The FDE-relevant donor lifetime at a specific distance obeys $\tau_{DA}(r) = (k_{rad} + k_T(r))^{-1}$ with high values of k_T implying small displacements. Indeed, it is common practice in FRET experiments to choose the FRET pairs such that their Förster radii, R_0, match the anticipated equilibrium distances. To further keep the FDE at a minimum, donors with short radiative lifetimes are required since $k_T \propto \tau_0^{-1}$ (cf. eq 21).

For a flexible chain in nonviscous solution, however, the FDE is always large and has to be included in the analysis. The short-lived donor FTrp, for instance, has an experimental lifetime of only 2 ns but a radiative lifetime of 20 ns ($\Phi_D \sim 0.10$). At negligible FRET probability, the displacement is 70 Å for D = 40 Å^2/ns and is still high, 11 Å, when the chain is less flexible, D = 1 Å^2/ns.

A robust and reliable route to reduce and vary the FDE in preparation of a global analysis is by external means, by adding a viscogen that reduces the diffusion coefficient. The remaining problem is that high concentrations of a viscogen such as ethylene glycol, propylene glycol, or sucrose could affect the equilibrium distance distribution; the analysis would again become cumbersome, ambiguous, and unsuitable for a large-scale investigation on polypeptide conformation and dynamics as a function of amino acid composition and sequence. The HSE simulations point to a simple test that can establish whether a viscogen affects only chain dynamics and not structure, a test that can be carried out by simple steady-state-fluorescence measurements.

The FDE Depends Symmetrically on Diffusion and Radiative Donor Lifetime. The random-walk perspective led us to speculate that the FDE might depend symmetrically on the diffusion coefficient and the donor lifetime and that both parameters could be used independently to control the FDE. Naturally, the time until the FRET donor−acceptor pair encounters regions of high FRET probability decreases with increasing diffusion, and the average donor lifetime, $\langle\tau_{DA}\rangle$, depends itself on the diffusion coefficient such that ΔR_{rms} =

dx.doi.org/10.1021/jp310381f | J. Phys. Chem. B 2013, 117, 185−198

$(6D\langle\tau_{DA}\rangle(D))^{1/2}$. As confirmed by simulation, the actual symmetry exists between the *radiative* lifetime and the diffusion coefficient and is a direct consequence of the specific form of the FRET distance law, $k_T = k_{rad}R_F^6/r^6$: The FDE-relevant donor lifetime at a specific distance follows $\tau_{DA}(r) = (k_{rad} + k_T)^{-1} = (k_{rad} + k_{rad}R_F^6/r^6)^{-1} = \tau_0(1 + R_F^6/r^6)$. Thus, also the average donor lifetime $\langle\tau_{DA}\rangle$ is proportional to the radiative lifetime: $\langle\tau_{DA}\rangle = (k_{rad} + \langle k_T\rangle)^{-1} = (k_{rad} + k_{rad}R_F^6\langle R_{DA}^{-6}\rangle)^{-1} = \tau_0(1 + R_F^6\langle R_{DA}^{-6}\rangle)$. We realize that changing the radiative lifetime leads to the same possible displacement, that is, the same FDE, as changing the diffusion coefficient in identical proportion. By substituting NAla for FTrp in the $(GS)_6$ chain, we changed the radiative lifetime from 256 to 19.6 ns, a decrease by a factor of 13.0. If we, instead, decrease the diffusion coefficient by the same factor (12.7) through a viscogen, we should monitor an identical R_{eff} and FDE value as after donor substitution (R_{eff} = 11.6 Å, Table 1). This is indeed the case, within error, when we used ethylene glycol (90% v/v) as a viscogen (R_{eff} = 11.2 Å, Table 1). If, upon coagent addition, the chain would collapse or expand, the effective distance would be much smaller or larger than after donor substitution. It seems that, even at high concentrations, ethylene glycol has only a very limited impact on chain structural propensities, which has already been of value in earlier studies on protein folding,[46,83] and provides now an experimental perspective for the exploratory results reported in Table 1.

Finally, we should relate time-resolved short-distance FRET to two complementary photophysical methods employed to assess the biopolymer chain dynamics: single-molecule FRET[25,84] and collision-induced quenching.[57,60,85,86] The donors used in short-distance FRET (FTrp and NAla) are unsuitable for single-molecule FRET due to their far-UV absorbance and low brightness, while the probes commonly used in single-molecule FRET are too large to be useful in monitoring short distances.[41] Collision-induced quenching, on the other hand, which is also limited by intrachain diffusion, differs formally from short-distance FRET in that an immediate contact between probe and quencher is a prerequisite, and it is a future challenge to compare these two methods.[87]

CONCLUSIONS

The structural and dynamic properties of *flexible* polypeptide chains have seen an immense increase in interest in regard to the refolding of globular proteins, the misfolding of amyloidogenic proteins, and the nonfolding of the intrinsically disordered proteins. Time-resolved FRET spectroscopy is a tool predestined to access dynamic and structural information on the chain. The decisive challenge is to delineate distance distribution and diffusion. We ventured into this project by working on the assumption, made on the basis of suggestions in the literature, that a systematic variation of the concentration of an external quencher could vary the relative proportion of diffusion-enhanced FRET. However, as demonstrated by experiment, theory, and simulations, this is not the case: The information content of FRET experiments depends on the radiative donor lifetime, yet the addition of external quencher does not alter this critical photophysical parameter. The insights which we have obtained are nevertheless of much experimental significance and fundamental for assessing mutual intrachain diffusion by FRET. First, experimental conditions to accurately characterize the initial distribution (plateau region in Figure 7c) and the chain mobility (linear region with negative slope in Figure 7c) would ideally need to involve variations of either the diffusion coefficient (viscosity) or the radiative donor lifetime, or the product of both, by 2 orders of magnitude. A variation in the observed donor lifetime or quantum yield alone, as it can be readily affected by the addition of an external quencher, varies neither of both critical parameters. Second, the effect of decreased donor quantum yield or quenched donor lifetime is opposite to what was originally expected: The effective donor−acceptor distance extracted from FRET decreases rather than increases in the presence of quencher (Figure 9c), while in the presence of diffusion, this effect becomes only obvious at very large quencher concentrations (or very low quantum yields). The large sensitivity of the effective donor−acceptor distance to the quantum yield of the employed donor for FRET pairs embedded in polydisperse polymer or biopolymer chains of limited or no mobility (or even of any mixture of two noninterconverting FRET systems of varying distance) has not been noted previously.

ASSOCIATED CONTENT

Supporting Information

Matlab files for HSE simulations are available from the authors upon request. Derivations of the quantum-yield dependence of the effective FRET parameters for a static equilibrium distance distribution, a rationalization for the pseudomonoexponential kinetics in time-resolved FRET measurements, and a list of symbols and abbreviations are available as Supporting Information. This material is available free of charge via the Internet at http://pubs.acs.org.

AUTHOR INFORMATION

Corresponding Author

*E-mail: m.jacob@jacobs-university.de (M.H.J.); w.nau@jacobs-university.de (W.M.N.).

Author Contributions

†Both authors contributed equally to this work.

Notes

The authors declare no competing financial interest.

ACKNOWLEDGMENTS

We would like to thank the Deutsche Forschungsgemeinschaft (DFG, NA 686/6) and the DAAD (doctoral fellowship for A.N.) for financial support. We are grateful to Attila Szabo and Eitan Lerner for their encouraging interest and for fruitful discussions. We respectfully dedicate this article to Izchak Z. Steinberg.

REFERENCES

(1) Grupi, A.; Haas, E. *J. Mol. Biol.* **2011**, *405*, 1267−1283.
(2) Grupi, A.; Haas, E. *J. Mol. Biol.* **2011**, *411*, 234−247.
(3) Ratner, V.; Kahana, E.; Haas, E. *J. Mol. Biol.* **2002**, *320*, 1135−1145.
(4) Haas, E. *ChemPhysChem* **2005**, *6*, 858−870.
(5) Jacob, M. H.; Amir, D.; Ratner, V.; Gussakowsky, E.; Haas, E. *Biochemistry* **2005**, *44*, 13664−13672.
(6) Ratner, V.; Amir, D.; Kahana, E.; Haas, E. *J. Mol. Biol.* **2005**, *352*, 683−699.
(7) Ittah, V.; Haas, E. *Biochemistry* **1995**, *34*, 4493−4506.
(8) Navon, A.; Ittah, V.; Landsman, P.; Scheraga, H. A.; Haas, E. *Biochemistry* **2001**, *40*, 105−118.
(9) Sinev, M. A.; Sineva, E. V.; Ittah, V.; Haas, E. *Biochemistry* **1996**, *35*, 6425−6437.
(10) Orevi, T.; Ben Ishay, E.; Pirchi, M.; Jacob, M. H.; Amir, D.; Haas, E. *J. Mol. Biol.* **2009**, *385*, 1230−1242.
(11) Wright, P. E.; Dyson, H. J. *J. Mol. Biol.* **1999**, *293*, 321−331.

(12) Avbelj, F.; Grdadolnik, S. G.; Grdadolnik, J.; Baldwin, R. L. *Proc. Natl. Acad. Sci. U.S.A.* **2006**, *103*, 1272−1277.
(13) Schweitzer-Stenner, R. *Mol. BioSyst.* **2012**, *8*, 122−133.
(14) Magg, C.; Schmid, F. X. *J. Mol. Biol.* **2004**, *335*, 1309−1323.
(15) Sinha, K. K.; Udgaonkar, J. B. *J. Mol. Biol.* **2007**, *370*, 385−405.
(16) Dasgupta, A.; Udgaonkar, J. B. *J. Mol. Biol.* **2010**, *403*, 430−445.
(17) Sarkar, S. S.; Udgaonkar, J. B.; Krishnamoorthy, G. *J. Phys. Chem. B* **2011**, *115*, 7479−7486.
(18) Schuler, B.; Lipman, E. A.; Eaton, W. A. *Nature* **2002**, *419*, 743−747.
(19) Schuler, B.; Eaton, W. A. *Curr. Opin. Struct. Biol.* **2008**, *18*, 16−26.
(20) Lipman, E. A.; Schuler, B.; Bakajin, O.; Eaton, W. A. *Science* **2003**, *301*, 1233−1235.
(21) Schuler, B.; Lipman, E. A.; Steinbach, P. J.; Kumke, M.; Eaton, W. A. *Proc. Natl. Acad. Sci. U.S.A.* **2005**, *102*, 2754−2759.
(22) Gopich, I. V.; Szabo, A. *Proc. Natl. Acad. Sci. U.S.A.* **2012**, *109*, 7747−7752.
(23) Klostermeier, D.; Millar, D. P. *Biopolymers* **2001**, *61*, 159−179.
(24) Kahra, D.; Kovermann, M.; Low, C.; Hirschfeld, V.; Haupt, C.; Balbach, J.; Hübner, C. G. *J. Mol. Biol.* **2011**, *411*, 781−790.
(25) Nettels, D.; Gopich, I. V.; Hoffmann, A.; Schuler, B. *Proc. Natl. Acad. Sci. U.S.A.* **2007**, *104*, 2655−2660.
(26) Steinberg, I. Z.; Katchalski-Katzir, E. *J. Chem. Phys.* **1968**, *48*, 2404−2410.
(27) Haas, E.; Katchalski-Katzir, E.; Steinberg, I. Z. *Biopolymers* **1978**, *17*, 11−31.
(28) Beechem, J. M.; Haas, E. *Biophys. J.* **1989**, *55*, 1225−1236.
(29) Steinberg, I. Z. *J. Theor. Biol.* **1994**, *166*, 173−187.
(30) Haas, E.; Wilchek, M.; Katchalski-Katzir, E.; Steinberg, I. Z. *Proc. Natl. Acad. Sci. U.S.A.* **1975**, *72*, 1807−1811.
(31) Lakowicz, J. R.; Gryczynski, I.; Kusba, J.; Wiczk, W.; Szmacinski, H.; Johnson, M. L. *Photochem. Photobiol.* **1994**, *59*, 16−29.
(32) Kusba, J.; Lakowicz, J. R. *Methods Enzymol.* **1994**, *240*, 216−262.
(33) Kusba, J.; Piszczek, G.; Gryczynski, I.; Johnson, M. L.; Lakowicz, J. R. *Chem. Phys. Lett.* **2000**, *319*, 661−668.
(34) Lakowicz, J. R.; Kusba, J.; Gryczynski, I.; Wiczk, W.; Szmacinski, H.; Johnson, M. L. *J. Phys. Chem.* **1991**, *95*, 9654−9660.
(35) Berg, H. C. *Random Walks in Biology*; Princeton University Press: Princeton, NJ, 1993.
(36) Lakowicz, J. R. *Principles of Fluorescence Spectroscopy*, 3rd ed.; Kluwer Academic/Plenum: New York, 2006; p 498.
(37) Makarov, D. E.; Plaxco, K. W. *J. Chem. Phys.* **2009**, *131*, No. 085105.
(38) Möglich, A.; Joder, K.; Kiefhaber, T. *Proc. Natl. Acad. Sci. U.S.A.* **2006**, *103*, 12394−12399.
(39) Sahoo, H.; Roccatano, D.; Zacharias, M.; Nau, W. M. *J. Am. Chem. Soc.* **2006**, *128*, 8118−8119.
(40) Sahoo, H.; Nau, W. M. *ChemBioChem* **2007**, *8*, 567−573.
(41) Sahoo, H.; Roccatano, D.; Hennig, A.; Nau, W. M. *J. Am. Chem. Soc.* **2007**, *129*, 9762−9772.
(42) Jacob, M. H.; Nau, W. M. In *Folding, Misfolding and Nonfolding of Peptides and Small Proteins*; Schweitzer-Stenner, R., Ed.; John Wiley & Sons: Hoboken, NJ, 2011.
(43) Verbaro, D.; Ghosh, I.; Nau, W. M.; Schweitzer-Stenner, R. *J. Phys. Chem. B* **2010**, *114*, 17201−17208.
(44) Hudgins, R. R.; Huang, F.; Gramlich, G.; Nau, W. M. *J. Am. Chem. Soc.* **2002**, *124*, 556−564.
(45) Nau, W. M.; Huang, F.; Wang, X.; Bakirci, H.; Gramlich, G.; Marquez, C. *Chimia* **2003**, *57*, 161−167.
(46) Jacob, M.; Schindler, T.; Balbach, J.; Schmid, F. X. *Proc. Natl. Acad. Sci. U.S.A.* **1997**, *94*, 5622−5627.
(47) Jerome, F. S.; Tseng, J. T.; Fan, L. T. *J. Chem. Eng. Data* **1968**, *13*, 496.
(48) Schuler, B.; Kremer, W.; Kalbitzer, H. R.; Jaenicke, R. *Biochemistry* **2002**, *41*, 11670−11680.
(49) Naganathan, A. N.; Perez-Jimenez, R.; Sanchez-Ruiz, J. M.; Munoz, V. *Biochemistry* **2005**, *44*, 7435−7449.
(50) Eftink, M. R.; Jia, Y. W.; Hu, D.; Ghiron, C. A. *J. Phys. Chem.* **1995**, *99*, 5713−5723.
(51) Joshi, S.; Ghosh, I.; Pokhrel, S.; Madler, L.; Nau, W. M. *ACS Nano* **2012**, *6*, 5668−79.
(52) Khan, Y. R.; Dykstra, T. E.; Scholes, G. D. *Chem. Phys. Lett.* **2008**, *461*, 305−309.
(53) Förster, T. *Ann. Phys.* **1948**, *2*, 55−75.
(54) Lakowicz, J. R. *Principles of Fluorescence Spectroscopy*, 3rd ed.; Kluwer Academic/Plenum: New York, 2006; p 142.
(55) Liu, T.; Callis, P. R.; Hesp, B. H.; de Groot, M.; Buma, W. J.; Broos, J. *J. Am. Chem. Soc.* **2005**, *127*, 4104−4113.
(56) Sarkar, S. S.; Udgaonkar, J. B.; Krishnamoorthy, G. *J. Phys. Chem. B* **2011**, *115*, 7479−7486.
(57) Bieri, O.; Wirz, J.; Hellrung, B.; Schutkowski, M.; Drewello, M.; Kiefhaber, T. *Proc. Natl. Acad. Sci. U.S.A.* **1999**, *96*, 9597−601.
(58) Krieger, F.; Fierz, B.; Bieri, O.; Drewello, M.; Kiefhaber, T. *J. Mol. Biol.* **2003**, *332*, 265−274.
(59) Fierz, B.; Joder, K.; Krieger, F.; Kiefhaber, T. *Methods Mol. Biol.* **2007**, *350*, 169−187.
(60) Neuweiler, H.; Lollmann, M.; Doose, S.; Sauer, M. *J. Mol. Biol.* **2007**, *365*, 856−869.
(61) Möglich, A.; Joder, K.; Kiefhaber, T. *Proc. Natl. Acad. Sci. U.S.A.* **2008**, *105*, 6787.
(62) Lakowicz, J. R. *Principles of Fluorescence Spectroscopy*, 3rd ed.; Kluwer Academic/Plenum: New York, 2006; p 445.
(63) Steinberg, I. Z.; Haas, E.; Katchalski-Katzir, E. In *Time Resolved Spectroscopy in Biology*; Cundall, R. B., Dale, R. E., Eds.; Plenum Publishing: New York, 1983; pp 411−415.
(64) Haas, E. In *Protein Folding Handbook*; Buchner, J., Kiefhaber, T., Eds.; John Wiley & Sons: Hoboken, NJ, 2008.
(65) Klan, P.; Wirz, J. *Photochemistry of Organic Compounds*; Wiley: New York, 2009.
(66) Plaxco, K. W.; Uzawa, T.; Cheng, R. R.; Cash, K. J.; Makarov, D. E. *Biophys. J.* **2009**, *97*, 205−210.
(67) Collins, K. D.; Neilson, G. W.; Enderby, J. E. *Biophys. Chem.* **2007**, *128*, 95−104.
(68) Santoro, M. M.; Bolen, D. W. *Biochemistry* **1988**, *27*, 8063−8068.
(69) Jacob, M. H.; Saudan, C.; Holtermann, G.; Martin, A.; Perl, D.; Merbach, A. E.; Schmid, F. X. *J. Mol. Biol.* **2002**, *318*, 837−45.
(70) Bicout, D. J.; Szabo, A. *Protein Sci.* **2000**, *9*, 452−465.
(71) Roccatano, D.; Sahoo, H.; Zacharias, M.; Nau, W. M. *J. Phys. Chem. B* **2007**, *111*, 2639−2646.
(72) The combination of both "diffusion-suppressing" strategies, i.e., the use of the short-lived donor in a highly viscous solution, led to an increase in R_{eff} by ca. 6 Å (see last entry in Table 1); the "true" R_{eff} value (in the absence of any FDE) is still expected to be larger, and we are trying to reach the limit in an ongoing experimental project.
(73) Huang, F.; Rajagopalan, S.; Settanni, G.; Marsh, R. J.; Armoogum, D. A.; Nicolaou, N.; Bain, A. J.; Lerner, E.; Haas, E.; Ying, L. M.; Fersht, A. R. *Proc. Natl. Acad. Sci. U.S.A.* **2009**, *106*, 20758−20763.
(74) Nettels, D.; Hoffmann, A.; Schuler, B. *J. Phys. Chem. B* **2008**, *112*, 6137−6146.
(75) Lapidus, L. J.; Eaton, W. A.; Hofrichter, J. *J. Mol. Biol.* **2002**, *319*, 19−25.
(76) Soranno, A.; Longhi, R.; Bellini, T.; Buscaglia, M. *Biophys. J.* **2009**, *96*, 1515−1528.
(77) Thirumalai, D.; Ha, B.-Y. In *Theoretical and Mathematical Models in Polymer Research*; Grossberg, A., Ed.; Academic: New York, 1998; pp 1−35.
(78) May, V.; Kühn, O. *Charge and Energy Transfer Dynamics in Molecular Systems*; Wiley-VCH: Berlin, 2000.
(79) Sridevi, K.; Udgaonkar, J. B. *Biochemistry* **2003**, *42*, 1551−1563.
(80) Sinha, K. K.; Udgaonkar, J. B. *J. Mol. Biol.* **2005**, *353*, 704−718.
(81) Lapidus, L. J.; Steinbach, P. J.; Eaton, W. A.; Szabo, A.; Hofrichter, J. *J. Phys. Chem. B* **2002**, *106*, 11628−11640.
(82) Ingratta, M.; Duhamel, J. *J. Phys. Chem. B* **2008**, *112*, 9209−9218.

(83) Jacob, M.; Geeves, M.; Holtermann, G.; Schmid, F. X. *Nat. Struct. Biol.* **1999**, *6*, 923−926.
(84) Neuweiler, H.; Schulz, A.; Bohmer, M.; Enderlein, J.; Sauer, M. *J. Am. Chem. Soc.* **2003**, *125*, 5324−5330.
(85) Huang, F.; Nau, W. M. *Angew. Chem., Int. Ed.* **2003**, *42*, 2269−72.
(86) Lapidus, L. J.; Eaton, W. A.; Hofrichter, J. *Proc. Natl. Acad. Sci. U.S.A.* **2000**, *97*, 7220−7225.
(87) When the monoexponential FTrp decay lifetimes (Table 1) are employed to calculate an apparent quenching rate constant from the short-distance FRET experiments, the resulting values are up to 1 order of magnitude faster than the rate constants extracted from collsion-induced quenching experiments for the same peptides (ref 44) or the same peptide backbone (ref 58).